



Nair, M., Ahmed, Q. Z., Wang, J., & Zhu, H. (2017). Low-Complexity Hybrid Digital-to-Analog Beamforming for Millimeter-Wave Systems with High User Density. In *2017 IEEE 85th Vehicular Technology Conference (VTC Spring 2017)* (pp. 1096-1100). Institute of Electrical and Electronics Engineers (IEEE).
<https://doi.org/10.1109/VTCSpring.2017.8108384>

Peer reviewed version

Link to published version (if available):
[10.1109/VTCSpring.2017.8108384](https://doi.org/10.1109/VTCSpring.2017.8108384)

[Link to publication record in Explore Bristol Research](#)
PDF-document

This is the author accepted manuscript (AAM). The final published version (version of record) is available online via IEEE at <https://ieeexplore.ieee.org/document/8108384> . Please refer to any applicable terms of use of the publisher.

University of Bristol - Explore Bristol Research

General rights

This document is made available in accordance with publisher policies. Please cite only the published version using the reference above. Full terms of use are available:
<http://www.bristol.ac.uk/red/research-policy/pure/user-guides/ebr-terms/>

Low-Complexity Hybrid Digital-to-Analog Beamforming for Millimeter-Wave Systems with High User Density

Manish Nair¹, Qasim Zeeshan Ahmed², Junyuan Wang¹ and Huiling Zhu¹

¹School of Engineering and Digital Arts, University of Kent, Canterbury, CT2 7NT, United Kingdom.

²University of Huddersfield, Queensgate, Huddersfield, HD1 3DH, United Kingdom.

Email: {mn307, jw712 and h.zhu}@kent.ac.uk, ¹q.ahmed@hud.ac.uk

Abstract—Supporting high user density and improving millimeter-wave (mm-Wave) spectral-efficiency (SE) is imperative in 5G systems. Current hybrid digital-to-analog beamforming (D-A BF) base stations (BS) can only support a particular user per radio frequency (RF) chain, which severely restricts mm-Wave SE. In this paper a novel low-complexity selection combining (LC-SC) is proposed for supporting high user density for mm-Wave BS. When compared with the current state of the art hybrid D-A BF, simulations show that LC-SC can support high user density and attain higher SE.

I. INTRODUCTION

Millimeter-wave (mm-Wave) cellular bands can significantly enhance spectral efficiency (SE) in 5G cellular systems [1]. A complete digital system having radio frequency (RF) transceiver chain per antenna (ANT) element cannot be implemented in base stations (BS) at mm-Wave due to the cost and complexity [2]. A practical 5G BS deploys a small number of RF chains with each RF chain supporting a massive number of transmit (Tx) antennas, resulting in hybrid digital-to analog beamforming (D-A BF) [3].

For the hybrid D-A BF BS schemes proposed in [4], [5], the digital beamformer is identity and the analog beamformer is the channel hermitian. However, the major drawback in this type of hybrid D-A BF structure is that each RF chain can only support a particular user, and the maximum number of users that can be supported by the BS cannot exceed the number of RF chains [4]. This will severely limit the SE of the future mm-Wave 5G environments such as train stations, stadiums or shopping malls. Therefore, it is of paramount necessity to design new hybrid D-A BF schemes which can support multiple users by employing a single RF chain and achieve similar SE as in the hybrid D-A BF techniques proposed in [4], [5]. Superposition coding can be applied to the Tx symbols on a single stream to support multiple users through a RF chain. However, it cannot serve multiple users simultaneously as only a single 3 dimensional (3D) beam is formed [6].

In this paper, a new hybrid D-A BF algorithm for supporting high user density is proposed, where each user will have its own separate 3D beam. This algorithm is the low-complexity selection combining (LC-SC). Our proposed hybrid D-A BF algorithm also accounts for the 3D mm-Wave channel for a high user density mm-Wave system which is generated when planar antenna (ANT) arrays are employed [7]. LC-SC is a space-time analog beamforming (A-BF) technique which modifies the A-BF matrix by designating a set of antenna elements to each user. The users and antennas are selected

depending upon their instantaneous channel state information (CSI).

Simulation results corroborate that the proposed hybrid D-A BFs using LC-SC algorithm achieves superior SE compared to other hybrid D-A BF algorithms as proposed in [4], [5].

The reminder of this paper is organized as follows. Section II describes the system model. In Section III, the hybrid D-A BF LC-SC algorithm is proposed. Section IV presents the simulation results. The paper is concluded in Section VI. Throughout this paper, upper case and lower case boldfaces are used for matrices and vectors, respectively. \mathbf{X} , \mathbf{X}^T , \mathbf{X}^H denote a matrix transpose and hermitian respectively. $\|\cdot\|$ and $\|\cdot\|_F$ represents the norm and Frobenius norm, respectively. Lastly, \mathbf{I} is the identity matrix.

II. DESCRIPTION OF THE HYBRID D-A BF SYSTEM

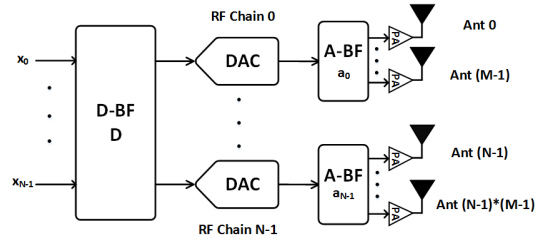


Figure 1. Hybrid BF Structure

The block diagram of the current hybrid D-A BF BS system is shown in Fig. 1 [4], [5]. Each of the N RF chains is connected to a large-scale array of M identical antennas. In this paper, the analysis is initially carried out considering a downlink scenario for an i -th RF chain supporting only a particular k -th user, where $0 < i \leq N-1$ and $0 < k \leq K-1$. Subsequently, two hybrid D-A BF algorithms, LC-SC and PC, are considered for scaling-up the number of users supported by the i -th RF chain by K , where $K \leq M$. Furthermore, for the i -th RF chain, the A-BF is performed over M antennas and L time-slots by the space-time analog beamformer $\mathbf{a}_i(t)$. The complete digital beamformer $\mathbf{D} = \text{diag}[d_1, d_2, \dots, d_N]$ is an $N \times N$ matrix accounting for all N RF chains of the BS.

A. 3D mm-Wave Modified SV Channel Model

The 3D mm-wave modified Saleh-Valenzuela (SV) channel modeled by L multi-path coefficients [8–14] is given by

$$\begin{aligned} h_{i,m,k}(t) &= \sum_{v=0}^{V-1} \sum_{u=0}^{U-1} \beta_{i,m,uv,k} h_{i,m,uv,k}(t - \tau_v - \tau_{uv}) \\ &= \sum_{l=0}^{L-1} \beta_{i,m,l,k} h_{i,m,l,k}(t - l\tau), \end{aligned} \quad (1)$$

where $h_{i,m,l,k}$ is the k -th user convolutional impulse response (CIR) of l -th resolvable multi-path for the m -th Tx antenna in the i -th RF chain. V denotes the number of clusters, U the number of of resolvable multi-path in one cluster, and $L = UV$ is the total number of resolvable multi-paths at the receiver. l is related to u and v by $l = vU + u$. $h_{i,m,uv,k} = |h_{i,m,uv,k}|e^{j\theta_{uv}}$ represents the fading gain of the u -th resolvable multi-path in the v -th cluster connecting the m -th antenna in the i -th RF chain to the k -th user. τ_v is the time-of-arrival (ToA) of the v -th cluster and $\tau_{uv} = u\tau$ denotes the ToA of the u -th resolvable multi-path in the v -th cluster. In our mm-Wave channel, it is assumed that the average power of a multi-path at a given delay is related to the power of the first resolvable multi-path of the first cluster through the following relationship [9], [10]

$$P_{uv}^k = P_{00}^k \exp\left(-\frac{\tau_v}{\Psi}\right) \exp\left(-\frac{\tau_{uv}}{\psi}\right), \quad (2)$$

where $P_{uv}^k = P_l^k = |h_{i,m,uv,k}|^2$ represents the expected power of the u -th resolvable multi-path in the v -th cluster connecting the k -th user to the m -th antenna in the i -th RF chain. Ψ and ψ are the corresponding power delay constants of the cluster and the resolvable multi-path respectively. For the channel model to be generic, we assume that the delay spread, which is $(L-1)\tau$ for the mm-Wave channel, spans $g \geq 1$ data bits, satisfying $(g-1)N_\tau \leq (L-1)\tau \leq gN_\tau$, where N_τ is the number of time slots per symbol [9], [10]. Secondly, we assume that the L resolvable multi-path components are randomly distributed and does not change over each symbol. Due to the wide bandwidth at mm-Wave, all the L multi-path components can be potentially resolved at the receiver (Rx) side [15]. Lastly, the k -th user's 3D BF gain $\beta_{i,m,uv,k} = \beta_{i,m,l,k}$ for the m -th Tx antenna of the i -th RF chain is given in (3) shown at the bottom of this page. In (3), $F_{Rx,V}$ and $F_{Rx,H}$ are the Rx antenna radiation patterns for the vertical (V) and horizontal (H) polarizations, respectively. $F_{Tx,i,V}$ and $F_{Tx,i,H}$ are the corresponding vertical (V) and horizontal (H) polarizations for the i -th RF chain. $\phi_l^{VV}, \phi_l^{VH}, \phi_l^{HV}, \phi_l^{HH}$ are the initial random phases for vertical (VV), cross (VH, HV), and horizontal polarizations (HH) for the l -th multi-path. κ_m is the intra-cluster Rician K -factor associated with the m -th Tx antenna cluster. ϑ_l and φ_l are the elevation and azimuth angle-of-arrival (AoA), respectively at the k -th user. Finally, $\theta_{l,m}$ and

$\phi_{l,m}$ are the elevation and azimuth angle-of-departure (AoD) of the l -th resolvable multi-path from the m -th Tx antenna in the i -th RF chain.

B. Received Symbols of the Hybrid D-A BF System

The k -th user $L \times 1$ received symbol vector is given by

$$\mathbf{y}_{i,k}(t) = \mathbf{H}_{i,k}(t)\mathbf{z}_i(t) + \mathbf{n}_{i,k}(t), \quad (4)$$

where $\mathbf{H}_{i,k}(t)$ is the $L \times M(2L-1)$ space-time channel matrix associating the i -th RF chain having M Tx antennas with k -th user given by (6) in the following page. In (6), $\mathbf{H}_{i,m,k}(t)$ is the $L \times (2L-1)$ Block-Toeplitz space-time CIR matrix associating the m -th Tx antenna of the i -th RF chain with the k -th user, and is given by (7). In (4) $\mathbf{z}_i(t) = [z_0(t), z_1(t-1), \dots, z_{L-1}(t-L+1)]^T$ is the $M(2L-1) \times 1$ beamformed data symbol vector associated with the i -th RF chain. $\mathbf{n}_{i,k}(t)$ is the $L \times 1$ complex Gaussian channel vector with a co-variance of $2\sigma_i^2 \mathbf{I}$ for the k -th user.

C. Space-Time Analog Beamformer for the mm-Wave Hybrid D-A BF System

The beamformed data vector $\mathbf{z}_i(t)$ in (4) is generated by the $M(2L-1) \times 1$ space-time analog beamformer $\mathbf{a}_i(t)$ operating over the $L \times M(2L-1)$ space-time channel matrix $\mathbf{H}_{i,k}(t)$ as well as the information bearing symbol $x_{i,k}(t)$ with $\mathbb{E}[x_{i,k}x_{i,k}^H] = \gamma_0$, where γ_0 is the expected transmitted symbol power. $x_{i,k}$ is given by

$$\mathbf{z}_i(t) = \mathbf{a}_i(t)d_i x_{i,k}(t), \quad (5)$$

where d_i is the i -th element of the D-BF matrix in Fig. 1 which corresponds to the i -th RF chain of the BS. The D-BF matrix is initially taken as identity [4], [5]. Therefore in (5), $d_i = 1$. $\mathbf{a}_i(t)$ is the $M(2L-1) \times 1$ our proposed novel space-time analog beamformer given by (8a), where the m -th element of $\mathbf{a}_i(t)$, denoted by $\mathbf{a}_{i,m}(t)$, is a normalized $(2L-1) \times 1$ vector given in (8b). The $L \times 1$ k -th user's Rx signal from the i -th RF chain is denoted by the vector $\mathbf{H}_{i,k}(t)\mathbf{a}_i(t)$ in (9). Lastly, the dimensions of (6) – (9) have been indicated by their respective under-braces.

D. Receive SNR and Spectral Efficiency for the Hybrid D-A BF System

The signal to noise ratio (SNR) of the i -th RF chain is denoted by γ_i and is given as [16]

$$\gamma_i(d_i, \mathbf{a}_i(t), \mathbf{H}_{i,k}(t)) = \frac{\gamma_0}{\sigma_i^2} \sum_{l=0}^{L-1} \|\mathbf{H}_{i,k}(t)\mathbf{a}_i(t)d_i\|^2 \quad (10)$$

The SE (bp/s/Hz) for the k -th user associated with the i -th RF chain can be obtained as [16]

$$\eta_{i,k} = \log_2[1 + \gamma_i(d_i, \mathbf{a}_i(t), \mathbf{H}_{i,k}(t))] \quad (11)$$

$$\beta_{i,m,l,k} = \sqrt{P_{l,k}} \begin{bmatrix} F_{Rx,V}(\varphi_l, \vartheta_l) \\ F_{Rx,H}(\varphi_l, \vartheta_l) \end{bmatrix}^T \begin{bmatrix} e^{j\phi_l^{VV}} & \sqrt{\kappa_m^{-1}} e^{j\phi_l^{VH}} \\ \sqrt{\kappa_m^{-1}} e^{j\phi_l^{HV}} & e^{j\phi_l^{HH}} \end{bmatrix} \begin{bmatrix} F_{Tx,i,V}(\phi_{l,m}, \theta_{l,m}) \\ F_{Tx,i,H}(\phi_{l,m}, \theta_{l,m}) \end{bmatrix} \quad (3)$$

$$\mathbf{H}_{i,k}(t) = [\mathbf{H}_{i,0,k}(t), \mathbf{H}_{i,1,k}(t), \dots, \mathbf{H}_{i,M-1,k}(t)] \quad (6)$$

$$= \begin{bmatrix} h_{i,m,0,k}(t) & h_{i,m,1,k}(t) & \dots & h_{i,m,L-1,k}(t) & 0 & \dots & 0 \\ 0 & h_{i,m,0,k}(t-1) & h_{i,m,1,k}(t-1) & \dots & h_{i,m,L-1,k}(t-1) & \dots & 0 \\ \vdots & \ddots & \ddots & \ddots & \ddots & \ddots & \vdots \\ 0 & \dots & 0 & h_{i,m,0,k}(t-L+1) & h_{i,m,1,k}(t-L+1) & \dots & h_{i,m,L-1,k}(t-L+1) \end{bmatrix} \quad (7)$$

$$\mathbf{a}_i(t) = \underbrace{[\mathbf{a}_{i,0}^T(t), \mathbf{a}_{i,1}^T(t), \dots, \mathbf{a}_{i,M-1}^T(t)]^T}_{M(2L-1) \times 1} \quad (8a)$$

$$\text{where } \mathbf{a}_{i,m}(t) = \underbrace{\begin{bmatrix} \underbrace{h_{i,m,0,k}^*(t)}_{t\text{-th time slot}} \underbrace{h_{i,m,1,k}^*(t-1)}_{t-1\text{-th time slot}} \dots \underbrace{h_{i,m,L-1,k}^*(t-L+1)}_{t-L+1\text{-th time slot}} \underbrace{0, \dots, 0}_{L-1 \text{ time slots}} \end{bmatrix}^T}_{(2L-1) \times 1} \underbrace{\frac{\sqrt{h_{i,0,0,k}^2(t) + h_{i,0,1,k}^2(t-1) + \dots + h_{i,0,L-1,k}^2(t-L+1)}}}{M-1}}_{M-1} \quad (8b)$$

$$\mathbf{H}_{i,k}(t)\mathbf{a}_i(t) = \sum_{m=0}^{M-1} \mathbf{H}_{i,m,k}(t)\mathbf{a}_{i,m}(t) \quad (9a)$$

$$= \begin{bmatrix} |h_{i,0,0,k}|^2 + \dots + |h_{i,0,L-1,k}|^2 + |h_{i,1,0,k}|^2 + \dots + |h_{i,1,L-1,k}|^2 + \dots + |h_{i,M-1,0,k}|^2 + \dots + |h_{i,M-1,L-1,k}|^2 \\ \frac{\sqrt{h_{i,0,0,k}^2(t) + h_{i,0,1,k}^2(t-1) + \dots + h_{i,0,L-1,k}^2(t-L+1)}}{h_{i,0,0,k}(t)h_{i,0,1,k}^*(t-1) + \dots + h_{i,0,L-2,k}(t)h_{i,0,L-1,k}^*(t-1) + \dots + h_{i,M-1,L-2,k}(t)h_{i,M-1,L-1,k}^*(t-1)} \\ \frac{\sqrt{h_{i,1,0,k}^2(t) + h_{i,1,1,k}^2(t-1) + \dots + h_{i,1,L-1,k}^2(t-L+1)}}{\vdots} \\ \frac{h_{i,0,0,k}(t)h_{i,0,L-1,k}^*(t-1) + h_{i,1,0,k}(t)h_{i,1,L-1,k}^*(t-1) + \dots + h_{i,M-1,0,k}(t)h_{i,M-1,L-1,k}^*(t-1)}{\sqrt{h_{i,1,M-1,k}^2(t) + h_{i,1,M-1,k}^2(t-1) + \dots + h_{i,M-1,L-1,k}^2(t-L+1)}} \end{bmatrix}^T \quad (9b)$$

III. BEAMFORMER DESIGN FOR HYBRID D-A BF

Suppose K users are to be supported by the i -th RF chain with M Tx antennas, where $K \leq M$. The allocation of antennas is based on the calculation of instantaneous power of the 3D mm-Wave modified SV channel for every user. For the m -th antenna in the i -th RF chain, the channel power associated with the k -th user is calculated as

$$p_{i,m,k} = \sum_{l=0}^{L-1} |h_{i,m,l,k}|^2, k = 1, \dots, K \quad (12)$$

The m -th antenna is then assigned to that user which has the maximum power, i.e.

$$k_m = \underset{k}{\operatorname{argmax}} \{p_{i,m,0}, p_{i,m,1}, \dots, p_{i,m,K-1}\} \quad (13)$$

This process is repeated M times until all the M antennas are allocated to the S users where $S \leq K$. The remaining $(K - S)$ users are not supported. Since S users are selected for the i -th RF chain, S continuous symbols from the i -th symbol stream have to be multiplexed. In this paper, we propose using S orthogonal time slots from the i -th symbol stream, to create S continuous symbol-streams for the selected s -th user. The resulting trade-offs in complexity and performance will be discussed in further detail in Section IV and Section V respectively.

As the LC-SC algorithm allocates non-contiguous antenna elements to the s -th user, it will experience multi-user interference (MUI) from the beamformed signals generated from antenna elements that are allocated to other users. MUI can be eliminated at every s -th user by the combination of mm-Wave SV channel effects and a set of simple Rx BF weights at every

s -th user. It is assumed that the LC-SC antenna allocation information is available at each user. For example, consider a scenario depicted in Fig. 2 in which:

- The number of antenna elements in the i -th RF chain is $M = 4$.
- The total number of single antenna users to be supported by this i -th RF chain is $S = 3$.
- The SC antenna allocation for the i -th RF chain that follows the pattern as shown in Fig. 2. In this scenario, antenna $m = 0$ is allocated to user $s = 0$; $m = 1$ and $m = 3$ to $s = 2$; and $m = 2$ to $s = 1$.

As shown in the Fig. 2, in order to implement this scenario, $S = 3$ orthogonal time slots from the i -th symbol stream corresponding to the i -th RF chain will be selected to create 3 continuous symbol-streams for each of the s -th user. LC-SC space-time A-BF $\mathbf{a}_{i,SC}(t)$ is then performed over each of the M antennas over L time slots. The LC-SC space-time A-BF matrix $\mathbf{a}_{i,SC}(t)$, specific to the system scenario depicted in Fig. 2, can be derived using a similar approach as previously applied in (8). It is given by (14), where $h_{i,m,l,s}^*(t)$ is the conjugate of the complex channel coefficient connecting the

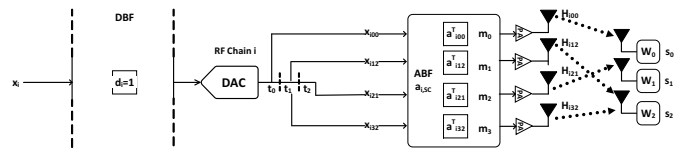


Figure 2. LC-SC antenna allocation for the i -th RF chain. t_0, t_1, t_2 and t_3 indicates the 0-th, 1-st, 2-nd and the 3-rd orthogonal time slots, or any 4 contiguous orthogonal time slots of the data stream \mathbf{x}_i which maps the i -th symbol stream onto the i -th RF chain. \mathbf{x}_{im_s} represents the symbol vector selected for the m -th antenna and the s -th user from the s -th time-slot in the i -th data stream \mathbf{x}_i

$$\mathbf{a}_{i,SC}(t) = \begin{bmatrix} \text{A-BF for 0-th ANT } m_0 & \text{A-BF for 1-st ANT } m_1 & \text{A-BF for 2-nd ANT } m_2 & \text{A-BF for 3-rd ANT } m_3 \end{bmatrix}^T$$

$$\text{where } \mathbf{a}_{i,m,s} = \begin{bmatrix} \mathbf{a}_{i,0,0}^T(t) & \mathbf{a}_{i,1,2}^T(t) & \mathbf{a}_{i,2,1}^T(t) & \mathbf{a}_{i,3,2}^T(t) \\ h_{i,m,0,s}^*(t), h_{i,m,1,s}^*(t-1), \dots, h_{i,m,L-1,s}^*(t-L+1), & 0, \dots, 0 \\ \hline \sqrt{h_{i,m,0,s}^2(t) + h_{i,m,1,s}^2(t-1) + \dots + h_{i,m,L-1,s}^2(t-L+1)} \end{bmatrix}^T$$

(2L-1) × 1 = 4(2L-1) × 1; i, m, s ∈ m-th Tx ANT allocated to s-th user from the i-th RF chain by LC-SC algorithm

$$\mathbf{H}_{i,2}(t) = \begin{bmatrix} \mathbf{H}_{i,0,2}(t), \mathbf{H}_{i,1,2}(t), \mathbf{H}_{i,2,2}(t), \mathbf{H}_{i,3,2}(t) \end{bmatrix}$$

L × M(2L-1) = L × 4(2L-1)

$$y_{i,2}(t) = \underbrace{\mathbf{w}\mathbf{H}_{i,0,2}(t)\mathbf{a}_{i,SC}(t)x_{i,0}(t)}_{\text{MUI at user } s=2 \text{ from user } s=0} + \underbrace{\mathbf{w}\mathbf{H}_{i,1,2}(t)\mathbf{a}_{i,SC}(t)x_{i,2}(t)}_{\text{MUI at user } s=2 \text{ from user } s=1} + \mathbf{w}\mathbf{H}_{i,2,2}(t)\mathbf{a}_{i,SC}(t)x_{i,1}(t) + \mathbf{w}\mathbf{H}_{i,3,2}(t)\mathbf{a}_{i,SC}(t)x_{i,2}(t) + \mathbf{w}\mathbf{n}_{i,2}(t) \quad (16)$$

$$\mathbf{H}_{i,2}(t)\mathbf{a}_{i,SC}(t) = \sum_{m=0}^{M=3} \mathbf{H}_{i,m,2}(t)\mathbf{a}_{i,m,SC}(t) \quad (17)$$

$$\mathbf{w}\mathbf{H}_{i,2}(t)\mathbf{a}_{i,SC}(t) = \begin{bmatrix} \underbrace{|h_{i,1,0,2}(t)|^2 + |h_{i,1,0,2}(t)|^2 + \dots + |h_{i,1,L-1,2}(t)|^2}_{L \text{ signal terms}} + \underbrace{|h_{i,3,0,2}(t)|^2 + \dots + |h_{i,3,L-1,2}(t)|^2}_{L \text{ signal terms}} \\ \hline \sqrt{h_{i,0,0,0}^2(t) + h_{i,0,1,0}^2(t-1) + \dots + h_{i,0,L-1,0}^2(t-L+1)} \\ \hline \underbrace{\text{Signal term of interest at user } s_2 \text{ at the } t\text{-th time-slot}}_0 \\ \vdots (L-3) \text{ zeros} \\ 0 \end{bmatrix}$$

L × 1

m-th Tx antenna element in the i-th RF chain via the l-th multi-path to the s-th user. It can be seen that $\mathbf{a}_{i,SC}(t)$ is a $4(2L-1)$ vector for the scenario depicted in Fig. 2.

As an example, let us examine specific the case for the $s = 2$ -nd user. The received symbol samples at the $s = 2$ -nd user is given by (16), where $\mathbf{H}_{i,m,s}(t)$ is the $L \times (2L-1)$ space-time CIR from the m-th Tx antenna in the i-th RF chain to the $s = 2$ -nd user. $x_{i,s}(t)$ is the Tx symbol from the i-th RF chain chosen for the s-th user from the 3 available orthogonal (in time) symbol streams, as shown in Fig. 2. $\mathbf{n}_{i,2}(t)$ is the $L \times 1$ complex Gaussian random noise for the user s_2 with a variance of $2\sigma_{i,2}^2\mathbf{I}$. The complete $L \times M(2L-1) = L \times 4(2L-1)$ space-time CIR, $\mathbf{H}_{i,2}$, connecting the i-th RF chain to the 2-nd user is given in (15). Similar to the discussion in Section II, the L symbol vectors, where each vector is sampled at the l-th time-slot by $s = 2$ -nd user, is denoted by $\mathbf{H}_{i,2}(t)\mathbf{a}_{i,SC}(t)$ and given in (17). In (17), similar to (9b), the first term sampled at the t-th time slot is the signal of interest at the $s = 2$ -nd user. The other terms are MUI components sampled over the remaining $t-1$ -th to $t-L+1$ -th time-slots. However, most of the MUI terms in (17) will be nearly zero. This is because of the exponentially decaying power delay profile of the mm-Wave SV channel given in (3). Additionally, in-order to eliminate the unwanted MUI terms over the $L-1$ time-slots, L Rx weights given by $\mathbf{w} = [1, 0, \dots, 0]$ can be applied. Therefore, in the $L \times 1$ received signal vector given in (18), the signal of interest at s_2 will be sampled only at the $l = 0$ -th time-slot. This analysis can be extended for any other LC-SC antenna allocation. In this way, the receiver complexity can be reduced significantly because processing is moved to the Tx side. To satisfy the total power constraint the signal power of the i-th RF chain is

$$\frac{1}{M} \sum_{m=1}^M \sum_{s=0}^{S-1} p_{i,m,s} \leq \sigma_i^2 \gamma_i \quad (19)$$

The SNR for the i-th RF chain and the s-th user for the LC-SC

algorithm is calculated as [16]

$$\gamma_{i,SC}(\mathbf{w}, d_i, \mathbf{a}_{i,SC}(t), \mathbf{H}_{i,s}(t)) = \frac{M_s \gamma_0}{SM} \sum_{l=0}^{L-1} \left\| (\sigma_{i,s}^2 \mathbf{w}^H)^{-1} \right. \\ \times \mathbf{w}^H \mathbf{H}_{i,s}^H(t) \mathbf{a}_{i,SC}^H(t) d_i^H \\ \left. \times d_i \mathbf{a}_{i,SC}(t) \mathbf{H}_{i,s}(t) \mathbf{w} \right\|, \quad (20)$$

where M_s is the number of antennas allocated to the s-th user and $\sigma_{i,s}^2$ is the corresponding noise variance. The overall sum SE for the i-th RF chain supporting S users is given by

$$\eta_{i,SC} = \sum_{s=0}^{S-1} \log_2 [1 + \gamma_i(\mathbf{a}_{i,SC}(t), \mathbf{H}_{i,s}(t))] \quad (21)$$

Lastly, the digital beamformer $\mathbf{D} = \mathbf{I}$ is an identity matrix of size N .

IV. SIMULATION RESULTS AND DISCUSSION

In this section, sum SE performance of two different kinds of hybrid D-A BF algorithms are investigated. The LC-SC based hybrid D-A BF is compared with the separate hybrid D-A BF [4], [5]. Perfect channel state information [17–28] is assumed. Two different environments are considered in our simulations. In the first environment perfect line-of-sight (LoS) is available. While, in the second environment, multi-path are present, and the number of resolvable multi-path is assumed to be 100 which accounts for a wideband SV mm-Wave channel. A uniform planar array of $M = 16 \times 16$ antennas is considered.

Fig. 3 shows the sum SE of this hybrid D-A BF system when using i-th RF chain. Fig. 3 indicates that by using the LC-SC algorithm to design the hybrid D-A BF system, the SE increases when the number of users per RF chain increases.

This is because with a larger number of users, the number of resolvable multi-path in the mm-Wave channel increases which are combined using A-BF to improve the SNR at the respective users. In this way, multi-path diversity has been exploited in our mm-Wave system. This is observed in the

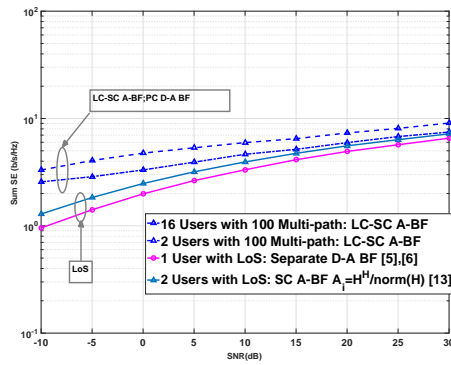


Figure 3. Sum SE of the proposed hybrid D-A BF systems. Results are reported for a downlink mm-Wave system with $M = 16 \times 16$ BS antennas from SNR of -30 dB to 30 dB. The simulated environment includes both a single LoS channel and $L = 100$ multi-path.

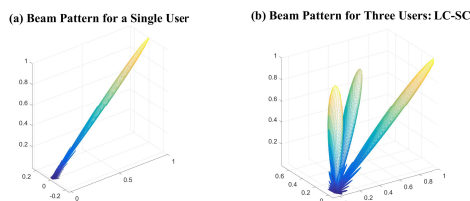


Figure 4. Normalized beam pattern for $M = 16 \times 16$ planar array using separate hybrid D-A BF design, LC-SC and PC. (a) Beam pattern of the original user in Separate Hybrid D-A BF Design. The angular location of the user is at $\theta = 0^\circ$ from the y - z plane $\phi = 30^\circ$ from the x - z plane, and (b) Hybrid D-A BF design using LC-SC. The combined beam patterns for the 3 users. The angular location of the 1-st user is unchanged, where as that of the 2-nd user is $\theta = 45^\circ$ from the y - z plane $\phi = 45^\circ$ from the x - z plane, and that of the 3-rd user is $\theta = 0^\circ$ from the y - z plane $\phi = 90^\circ$ from the x - z plane.

curves with 16 users and $L = 100$ resolvable multi-path per Tx antenna cluster attaining the upper bound as compared to the single user line-of-sight (LoS) case. 16 users per RF chain in a BS is chosen to represent a high user density scenario in mm-Wave systems. However, SE gains from multi-path diversity will be offset by the power constraint in the i -th RF chain, and it will tend to saturate. From this figure, it can also be observed that the LC-SC algorithm outperforms the benchmark separate hybrid D-A BF design in [4], [5]. Lastly, Fig. 6 plots the beam patterns generated by the $M = 16 \times 16$ planar BS antenna array in the i -th RF chain.

V. CONCLUSION

In this paper, a novel LC-SC algorithm has been proposed for hybrid D-A BF based mm-Wave system. From our based algorithm, it was possible to support more than a single user per RF chain. This algorithms have a significant impact when higher density of users were present and the particular RF chain had to support multiple users. From our simulations, it was observed that our proposed hybrid D-A BF using LC-SC achieves higher SE compared to the known hybrid D-A BF and supports higher density of users per RF chain.

ACKNOWLEDGEMENT

This work has received funding from the European Union's Horizon 2020 Research and Innovation Programme under Grant Agreement No. 643297 (RAPID: a Europe-Japan Collaboration).

REFERENCES

- [1] S. Sun, T. Rappaport, R. Heath, A. Nix, and S. Rangan, "MIMO for Millimeter-Wave Wireless Communications: Beamforming, Spatial multiplexing, or Both," *IEEE Communications Magazine*, vol. 52, no. 12, pp. 110–121, December 2014.
- [2] A. Alkhateeb, J. Mo, N. Gonzalez-Prelcic, and R. Heath, "MIMO Precoding and Combining Solutions for Millimeter-Wave Systems," *IEEE Communications Magazine*, vol. 52, no. 12, pp. 122–131, December 2014.
- [3] M. Crocco and A. Trucco, "Design of Superdirective Planar Arrays With Sparse Aperiodic Layouts for Processing Broadband Signals via 3-D Beamforming," *IEEE/ACM Transactions on Audio, Speech, and Language Processing*, vol. 22, no. 4, pp. 800–815, April 2014.
- [4] S. Han, C.-L. I, Z. Xu, and C. Rowell, "Large-Scale Antenna Systems with Hybrid Analog and Digital Beamforming for Millimeter Wave 5G," *IEEE Communications Magazine*, vol. 53, no. 1, pp. 186–194, January 2015.
- [5] W. Roh, J.-Y. Seol, J. Park, B. Lee, J. Lee, Y. Kim, J. Cho, K. Cheun, and F. Aryanfar, "Millimeter-Wave Beamforming as an Enabling Technology for 5G Cellular Communications: Theoretical Feasibility and Prototype Results," *IEEE Communications Magazine*, vol. 52, no. 2, pp. 106–113, February 2014.
- [6] H. T. Do and S. Y. Chung, "Linear beamforming and superposition coding with common information for the gaussian mimo broadcast channel," *IEEE Transactions on Communications*, vol. 57, no. 8, pp. 2484–2494, Aug 2009.
- [7] H. Xu, V. Kukshya, and T. Rappaport, "Spatial and Temporal Characteristics of 60-GHz Indoor Channels," *IEEE Journal on Selected Areas in Communications*, vol. 20, no. 3, pp. 620–630, Apr 2002.
- [8] O. El Ayach, S. Rajagopal, S. Abu-Surra, Z. Pi, and R. Heath, "Spatially Sparse Precoding in Millimeter Wave MIMO Systems," *IEEE Transactions on Wireless Communications*, vol. 13, no. 3, pp. 1499–1513, March 2014.
- [9] Q. Z. Ahmed, K. H. Park, M. S. Alouini, and S. Assa, "Compression and combining based on channel shortening and reduced-rank techniques for cooperative wireless sensor networks," *IEEE Transactions on Vehicular Technology*, vol. 63, no. 1, pp. 72–81, Jan 2014.
- [10] Q. Z. Ahmed and L. L. Yang, "Reduced-rank adaptive multiuser detection in hybrid direct-sequence time-hopping ultrawide bandwidth systems," *IEEE Transactions on Wireless Communications*, vol. 9, no. 1, pp. 156–167, January 2010.
- [11] M. Nair, Q. Z. Ahmed, and H. Zhu, "Hybrid digital-to-analog beamforming for millimeter-wave systems with high user density," in *2016 IEEE Global Communications Conference (GLOBECOM)*, Dec 2016, pp. 1–6.
- [12] O. Alluhaibi, Q. Z. Ahmed, C. Pan, and H. Zhu, "Capacity Maximisation for Hybrid Digital-to-Analog Beamforming mm-Wave Systems," to appear in *IEEE Global Communications Conference (GLOBECOM'16)*, Dec. 2016.
- [13] —, "Hybrid Digital-to-Analog Beamforming Approaches to Maximise the Capacity of mm-Wave Systems," to appear in *IEEE 85th Vehicular Technology Conference (VTC Spring)*, Jun. 2017.
- [14] O. Alluhaibi, Q. Z. Ahmed, J. Wang, and H. Zhu, "Hybrid Digital-to-Analog Precoding Design for mm-Wave Systems," to appear in *IEEE International Conference on Communications (ICC)*, May 2017.
- [15] A. Alkhateeb and R. W. Heath, "Frequency selective hybrid precoding for limited feedback millimeter wave systems," *IEEE Transactions on Communications*, vol. PP, no. 99, pp. 1–1, 2016.
- [16] A. Goldsmith, S. A. Jafar, N. Jindal, and S. Vishwanath, "Capacity limits of mimo channels," *IEEE Journal on Selected Areas in Communications*, vol. 21, no. 5, pp. 684–702, June 2003.
- [17] H. Zhu and J. Wang, "Chunk-based resource allocation in ofdma systems - part i: chunk allocation," *IEEE Transactions on Communications*, vol. 57, no. 9, pp. 2734–2744, September 2009.
- [18] —, "Chunk-based resource allocation in ofdma systems - part ii: Joint chunk, power and bit allocation," *IEEE Transactions on Communications*, vol. 60, no. 2, pp. 499–509, February 2012.
- [19] H. Zhu, "Radio resource allocation for ofdma systems in high speed environments," *IEEE Journal on Selected Areas in Communications*, vol. 30, no. 4, pp. 748–759, May 2012.
- [20] H. Zhu and J. Wang, "Performance analysis of chunk-based resource allocation in multi-cell ofdma systems," *IEEE Journal on Selected Areas in Communications*, vol. 32, no. 2, pp. 367–375, February 2014.
- [21] —, "Radio resource allocation in multiuser distributed antenna systems," *IEEE Journal on Selected Areas in Communications*, vol. 31, no. 10, pp. 2058–2066, October 2013.
- [22] H. Zhu, "On frequency reuse in cooperative distributed antenna systems," *IEEE Communications Magazine*, vol. 50, no. 4, pp. 85–89, April 2012.
- [23] H. Osman, H. Zhu, D. Tzoumpakis, and J. Wang, "Achievable rate evaluation of in-building distributed antenna systems," *IEEE Transactions on Wireless Communications*, vol. 12, no. 7, pp. 3510–3521, July 2013.
- [24] T. Alade, H. Zhu, and J. Wang, "Uplink spectral efficiency analysis of in-building distributed antenna systems," *IEEE Transactions on Wireless Communications*, vol. 14, no. 7, pp. 4063–4074, July 2015.
- [25] H. Zhu, "Performance comparison between distributed antenna and microcellular systems," *IEEE Journal on Selected Areas in Communications*, vol. 29, no. 6, pp. 1151–1163, June 2011.
- [26] J. Wang, H. Zhu, and N. J. Gomes, "Distributed antenna systems for mobile communications in high speed trains," *IEEE Journal on Selected Areas in Communications*, vol. 30, no. 4, pp. 675–683, May 2012.
- [27] H. Zhu, S. Karachontzitis, and D. Tzoumpakis, "Low-complexity resource allocation and its application to distributed antenna systems [coordinated and distributed mimo]," *IEEE Wireless Communications*, vol. 17, no. 3, pp. 44–50, June 2010.
- [28] R. Husbands, Q. Ahmed, and J. Wang, "Transmit antenna selection for massive MIMO: A knapsack problem formulation," to appear in *IEEE International Conference on Communications (ICC)*, vol. 57, no. 9, pp. 2734–2744, May 2017.